

Article

Comparison of Optical Ammonia-Sensing Properties of Conducting Polymer Complexes with Polysulfonic Acids

Oxana Gribkova ^{1,*}, Varvara Kabanova ¹, Vladimir Tverskoy ² and Alexander Nekrasov ¹

¹ A.N. Frumkin Institute of Physical Chemistry and Electrochemistry RAS, Leninskii Prospect 31, 119071 Moscow, Russia; kabanovavar@gmail.com (V.K.); alexander.nek@gmail.com (A.N.)

² Lomonosov Institute of Fine Chemical Technologies, MIREA—Russian Technological University, Vernadskogo Prospect 78, 119454 Moscow, Russia; tvorskoy@mitht.ru

* Correspondence: oxgribkova@gmail.com

Abstract: Thin films of conducting polymer complexes with polysulfonic acids of various structures were electrochemically deposited onto transparent FTO electrodes. The behavior of the polymer-based optical ammonia vapor sensors in response to various concentrations of ammonia vapors, ranging from 5 to 135 ppm, was investigated, including the response time and response amplitude. It was found that the nature of the conducting polymers (poly (3,4-ethylenedioxythiophene), polypyrrole, polyaniline), as well as the structure of the polyacids, affected the sensing performance of the obtained complexes.

Keywords: polyaniline; polypyrrole; PEDOT; electropolymerization; polyelectrolyte; ammonia-sensor



Citation: Gribkova, O.; Kabanova, V.; Tverskoy, V.; Nekrasov, A.

Comparison of Optical Ammonia-Sensing Properties of Conducting Polymer Complexes with Polysulfonic Acids. *Chemosensors* **2021**, *9*, 206. <https://doi.org/10.3390/chemosensors9080206>

Academic Editor: Boris Lakard

Received: 7 July 2021

Accepted: 30 July 2021

Published: 4 August 2021

Publisher's Note: MDPI stays neutral with regard to jurisdictional claims in published maps and institutional affiliations.



Copyright: © 2021 by the authors. Licensee MDPI, Basel, Switzerland. This article is an open access article distributed under the terms and conditions of the Creative Commons Attribution (CC BY) license (<https://creativecommons.org/licenses/by/4.0/>).

1. Introduction

Conducting polymers (CPs) are actively used as sensitive materials in gas sensors [1–4]. Sensors based on CP thin films have good mechanical properties and environmental stability, as well as high sensitivity to gases at room temperature [1–4]. Moreover, they can be easily synthesized through chemical or electrochemical polymerization of the monomers. Generally, the rapid reaction to various gases is caused by changes in the degree of CP oxidation, which is influenced by chemical oxidation/reduction. This effect leads to an immediate change in the conductivity and optical absorbance.

Sensing of ammonia gas, as one of the most widespread industrial pollutants, is of permanent interest to scientists in the field. The majority of ammonia sensors based on CP films operate via a chemiresistive transducing mechanism [1,2,5–7]. However, optical sensors can provide high sensitivity [8–10], fast response and simple regeneration [9], while their response is less influenced by electromagnetic interference, humidity and temperature [1,8–12]. Changes in the UV-visible-NIR spectra reflect the changes in electronic structure of CP upon exposure to ammonia gas. A thin film deposited on glass (or ITO glass) is suitable for the manufacture of an optical sensor, since spectral changes can be easily recorded using commercial spectrometers [1] or detected using single-wavelength optoelectronic pairs. Another advantage is the ability to transmit an analytical signal without distortion over long distances [1,12,13]. Despite the advantages described above, only a few studies have focused on the creation of CP-based optical ammonia sensors [8–14].

In the majority of studies devoted to CP-based ammonia sensors, the CPs were produced by chemical oxidative polymerization. Only in a few studies [3,13–16] were the sensing layers produced by electrodeposition, which makes it possible to obtain uniform films without residues of oxidants. With this method, the films can be deposited on metal, glass substrates with a transparent conductive layer (indium tin oxide (ITO) or fluorinated tin oxide (FTO)) and interdigitated microelectrodes. The films' thickness and morphology can be controlled by varying the electrosynthesis parameters (potential, current, charge spent for the synthesis, temperature, pH, etc.). Surface morphology and

internal spatial structure of CP films can be additionally controlled by introducing various polyelectrolytes into their structure [17–21]. The use of sulfonated polyelectrolytes during CP electrosynthesis leads to changes in their structure and properties (optical, electrochemical, spectroelectrochemical and morphological [16,22–28]). Also, important features of polyacids, as far as the stability of CP sensor characteristics is concerned, include the following: (1) they are not as volatile as HCl; and (2) their remnants inside the CP film after evaporation of the solvent are not as chemically aggressive as H₂SO₄ or HClO₄. To the best of our knowledge, the use of CP films electrodeposited in the presence of polysulfonic acids as gas sensors has never been considered. Earlier [16] polypyrrole complexes with different polyelectrolytes were first tested for optical ammonia sensing with a range of concentrations from 25 to 529 ppm.

In this work, we have reduced this range down to 5 ppm and performed a comparative study of the ammonia-sensing properties of interpolymer complexes of the most well-known CPs: polyaniline (PANI), polypyrrole (PPy) and poly(3,4-ethylenedioxythiophene) (PEDOT). Since PANI can be obtained only in acidic solutions, for adequate comparison we only investigated CP complexes with the acid form of polyelectrolytes. CP complexes with polysulfonic acids of different structures and chain flexibilities were electrodeposited on transparent FTO electrodes. The effects of the structure and flexibility of polyacids and of the nature of the CP on the mechanism of interaction between CP complexes and ammonia were considered.

2. Materials and Methods

2.1. Synthesis of Sensor Films

The electropolymerization of EDOT, pyrrole and aniline was carried out in the presence of the following polysulfonic acids (Figure 1): flexible-chain poly-2-acrylamido-2-methyl-1-propanesulfonic acid (PAMPSA) and poly(styrene-4-sulfonic) acid (PSSA); semi-rigid-chain poly-(4,4'-(2,2'-disulfoacid)-diphenylen-iso-phthalamide) (i-PASA); and rigid-chain poly-(4,4'-(2,2'-disulfoacid)-diphenylen-tere-phthalamide) (t-PASA). Laboratory-synthesized Na⁺-salts of i-PASA and t-PASA [29] (MW 40 000) and PSSNa (Aldrich, MW 1,000,000, 25% aqueous solution) were converted into H⁺-forms using an ion-exchange column. Then, along with PAMPSA (Aldrich, MW 2,000,000, 15% aqueous solution) they were purified via dialysis (cellulose membrane ZelluTrans MWCO 8000-, Roth) against deionized water for 3 days. The polyacids solutions were diluted by deionized water to the desired concentration and stirred for one day before use to provide homogenous mixing. The monomers were added into the polyacids' solutions by intensive stirring for 2 h.

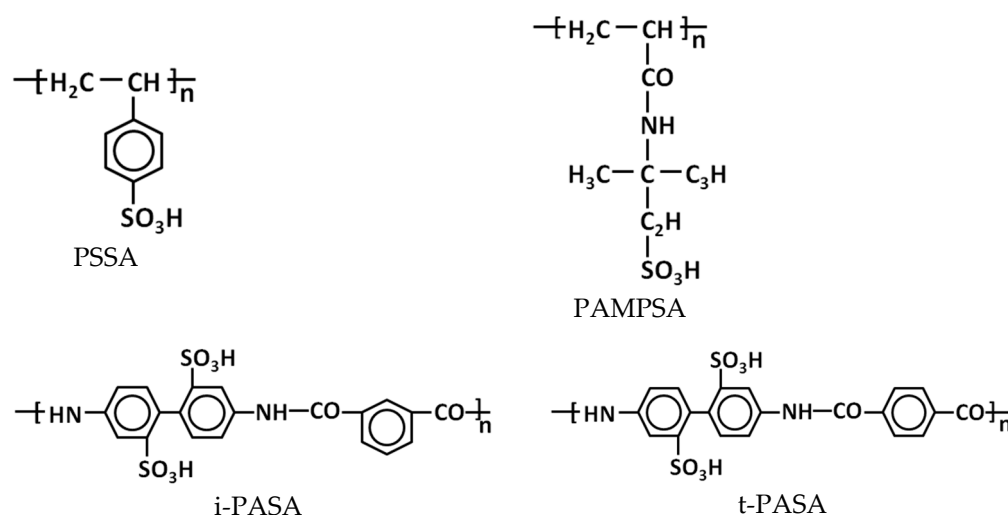


Figure 1. Chemical structure of constitutional units of polysulfonic acids used in the paper.

The conditions of electrosynthesis have been described in [23] for PEDOT, in [16,22] for PPy and in [24,25] for PANI. All syntheses were performed in the galvanostatic regime on glass substrates (8 × 40 mm) covered with a transparent conducting layer of SnO₂:F (FTO) with a sheet resistance of ca. 7 ohm/square. A platinum foil was used as a counter electrode and a saturated silver–silver chloride electrode (Ag/AgCl/KCl_{sat}) as a reference electrode. The concentrations of EDOT and pyrrole were 10 mM and that of aniline was 25 mM. The ratio of the concentrations of the monomer and sulfoacid groups was always kept as 0.5 mol to 1 g equivalent of the sulfoacid groups. The current densities were 50 μA/cm² for PEDOT, 100 μA/cm² for PPy and 20 μA/cm² for PANI. The surface area for all films was 2.0 cm². All the samples were thoroughly rinsed with deionized water after electrosynthesis and dried in air. The charge spent for the synthesis of CP films was 50 mC/cm². The thickness of CP polyacid films depending on the polyacid used were (nm): 150–250 (PANI), 200–300 (PEDOT) and 120–220 (PPy). The thicknesses of the films were measured with a MII-4 microinterferometer (LOMO, Russia).

2.2. Sensing Experiments and Instrumentation

The ammonia-sensing properties of CP films were studied as described in [16]. The films, electrodeposited on transparent FTO substrates, were placed in a closed 5 cm spectrophotometric quartz cell, filled with ammonia vapors in equilibrium (at 22–25 °C) with a 5 mm layer of the aqueous solutions of different NH₃ concentrations prepared through dilution of the 30% solution (Chimmed (Russia), analytical grade). The concentrations of ammonia in air (ppm) were calculated using an interpolated calibration curve based on the values for NH₃ partial pressure over ammonia aqueous solutions presented in [30]. UV-visible NIR (350–1000 nm) absorption spectra of CP films electrodeposited on FTO in air and exposed to the ammonia were registered using the AvaSpec 2048 spectrophotometer. The spectrum recording time was 2 s.

In general, the usability of a particular material as a sensor is determined by its sensitivity (detection limit) and response time, the concentration dependence of the response amplitude and the reversibility of changes in the measured parameter. In our case, this was the absorbance at the chosen wavelength(s) specific for each CP. Another criterion to choose these wavelengths is that they should be close to the standard wavelength of one of the light-emitting diodes, which can be used in optical pair detectors in practice instead of a spectrophotometer. The sensor response amplitude (ΔA) was calculated as:

$$\Delta A = \frac{A_{\text{NH}_3\text{vap}} - A_{\text{air}}}{A_{\text{air}}} 100\% \quad (1)$$

where $A_{\text{NH}_3\text{vap}}$ is the value of absorbance when the sample is exposed to NH₃ and A_{air} is the value of absorbance when the sample is exposed to air. The sensitivity in our case was determined as the minimum concentration of analyte causing a reproducible response amplitude of at least 2%. However, such low response amplitudes were observed only for CP complexes exhibiting the worst sensing performances at the minimum (5 ppm) content of ammonia used in this study.

The popular approach to determine the response time (t_r) using the results of response curve fitting (for example, by single or double exponents [31], Bessel's polynomial [32] or the reaction–diffusion model [33], etc.) is very useful if one compares the operation characteristics of a sensor based on a single polymer with varying thicknesses or morphologies, or with varying content of some additives (for example, carbon nanotubes). In our case, it was found that, due to the presence of polyelectrolytes in the acid form, a proton transporting network was formed in the bulk of the CP/PE films [16]. As a result, the shapes of the sensing responses of the CP complexes with the acid or salt forms of PEs were drastically different and could not be fitted with similar mathematic equations. Moreover, we compared the sensing responses of CPs with different sensing mechanisms, which also could not be fitted with similar equations. In order to obtain comparable results, we used another popular approach involving 90% of the response amplitude [2,8–10,13,14,16].

The measurement time in all cases was the same as the exposition time and equaled 800 s, which was considered as the maximum reasonable duration for practical application.

The diffusion coefficient (D) was calculated in accordance with Fick's second law [34]. For gas sorption occurring through one surface of the film, this equation is transformed into:

$$\frac{M_t}{M_k} = \frac{2}{l} \left(\frac{D_t}{\pi} \right)^{0.5} \quad (2)$$

where M_t is the amount of the sorbed or desorbed substance at the time t , M_k is the equilibrium amount of the sorbed substance and l is the film thickness.

This formula can be transformed to calculate the diffusion coefficient based on the time dependences of the optical absorption of the films during the sorption of ammonia:

$$\frac{A_t - A_0}{A_k - A_0} = \frac{2}{l} \left(\frac{D_t}{\pi} \right)^{0.5} \quad (3)$$

where A_0 and A_k are the optical absorbance at characteristic wavelengths in the initial and final moments of sensing, respectively and, A_t is the optical absorbance at a characteristic wavelength at time t .

The atomic force microscopic (AFM) images of CP films were recorded by using an Enviroscope with a Nanoscope V controller (all by Bruker) in tapping mode. The roughness of CP films was averaged from five different parts of three films.

Regeneration of the CP films after exposition to ammonia vapors by resistive heating of the FTO layer was tested. A current of 0.1 A was applied to the conducting layer of 8×40 mm, which caused heating of the layer up to ~ 75 °C.

3. Results and Discussion

3.1. Spectral Changes in CP Films during Exposition to Ammonia

Figure 2 shows the characteristic evolution of the optical absorption spectra of CP complexes with polyacids exposed to 52 ppm NH_3 .

In the case of PEDOT films, absorption growth in the region of 450–550 nm, corresponding to the reduced form of PEDOT [23,35], and a decrease of absorption in the region of 700–850 nm, corresponding to polarons [23,35], were observed (Figure 2a,b). Since NH_3 is an electron-donating molecule and PEDOT is not a pH-active CP, exposure of the PEDOT film to ammonia vapors led to an increase in the number of reduced fragments in the polymer chain [36,37]. In the case of the PEDOT complexes with flexible-chain polyacids, the optical changes were, in general, less noticeable but more pronounced in the range of 450–550 nm (Figure 2b). Therefore, for best comparison in the case of PEDOT, we studied the response transients at 500 nm (Figure 3a).

In the case of PPy (Figure 2c), the growth of absorption in the region around 420 nm (reduced form) and the decrease of absorption in the range greater than 800 nm (polarons), which corresponds to PPy reduction [38] or deprotonation [38,39], can be simultaneously seen. Two mechanisms for the interaction of ammonia with PPy have been proposed, based on electron transfer from ammonia to PPy [15] and proton transfer from PPy to ammonia [15,38]. A combination of these two mechanisms is also possible [38]. Since more noticeable changes in the absorption were observed in the NIR region, in the case of PPy we studied response transients at 850 nm (Figure 3b).

The changes of absorption in the PANI films are presented in Figure 2d. The decrease of absorption in the region around 800 nm, which is related to localized polarons, and at about 420 nm, which is related to the radical cations [40], can be seen. Simultaneously, the growth of absorption in the range of 550–650 nm, corresponding to the deprotonated form of PANI [9,40,41], can be observed. Such changes in the optical absorption spectra indicate the transition of PANI from a salt to a base form. Mutual transitions in the electronic structure of PANI were confirmed by the presence of two isobestic points. When PANI interacts with ammonia, the ammonia molecule takes up a proton from PANI, resulting in

the energetically more favorable NH_4^+ : $\text{PANI-H}^+ + \text{NH}_3 \rightarrow \text{PANI} + \text{NH}_4^+$ [10]. This leads to the dedoping (deprotonation) of PANI [9,10,42]. Due to fact that the changes in the range of 550–650 nm were more reproducible and more noticeable, we chose the wavelength of 600 nm to study the optical response transients of PANI films.

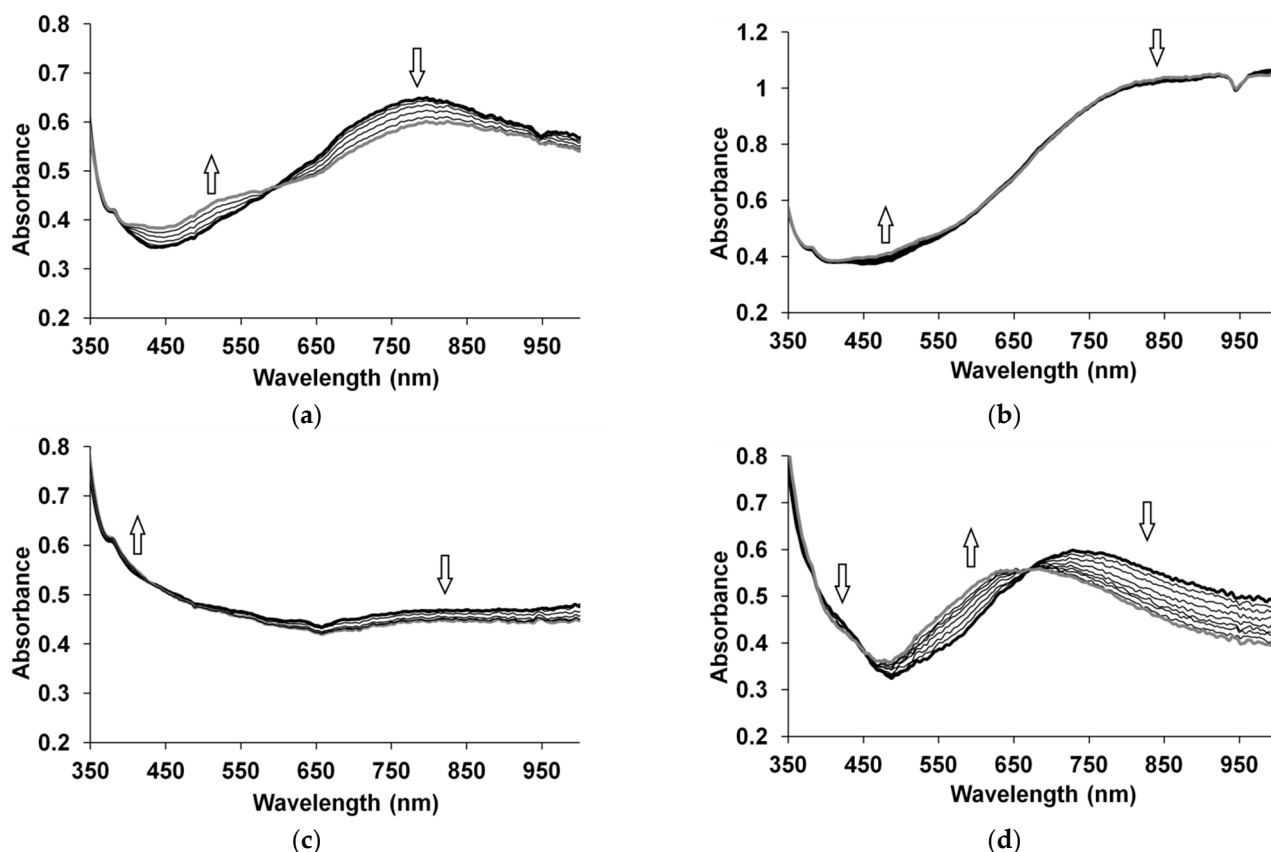


Figure 2. Evolution of UV-visible NIR absorption spectra of PEDOT-i-PASA (a), PEDOT-PSSA (b), PPy-i-PASA (c) and PANI-PAMPSA (d) exposed to 52 ppm NH_3 . Up (down) arrows indicate simultaneous growth (reduction) of absorbance at characteristic wavelengths during an 800 s exposure to ammonia vapor.

3.2. Sensing Properties

One can see in Figure 3a,b that the PEDOT and PPy complexes with rigid-chain polyacids demonstrated higher optical responses than their complexes with flexible-chain polyacids. In contrast, in the case of PANI (Figure 3c), the complex with flexible-chain PAMPSA had the highest response. PANI complexes with rigid-chain polyacids have slightly lower responses. Despite the very similar structures of i-PASA and t-PASA (Figure 1), PANI-t-PASA film demonstrated a certain induction period (the longest response time). It is interesting that the complexes of all the CPs with the popular polymeric dopant PSSA demonstrated the lowest response amplitudes.

Figure 4 shows the dependences of the maximum response amplitude (ΔA) at the characteristic wavelengths on the concentration of ammonia in air for the films of CP complexes with various polyacids. Nonlinear dependences were observed for all CP complexes with increased gradients at low concentrations (<52 ppm), whereas most of the dependences were saturated at higher ammonia concentrations.

Very similar shapes of optical response dependences on ammonia concentrations were observed in [10–12] and for chemiresistive response in [5,37]. In [5], nonlinear behavior in the range of 5–50 ppm was related to the adsorption of NH_3 vapor molecules on the surface of the PPy film. At the increased (50–200 ppm) concentrations of NH_3 , suggesting a decreasing number of active adsorption sites, a decrease in the slope of the response

concentration dependence was observed. In [37], it was supposed that, at the concentrations higher than 20 ppm, PEDOT films were saturated with NH_3 . The authors of [11] suggested the combined influence of the adsorption/diffusion/desorption of ammonia in the PANI layer on the sensing performance.

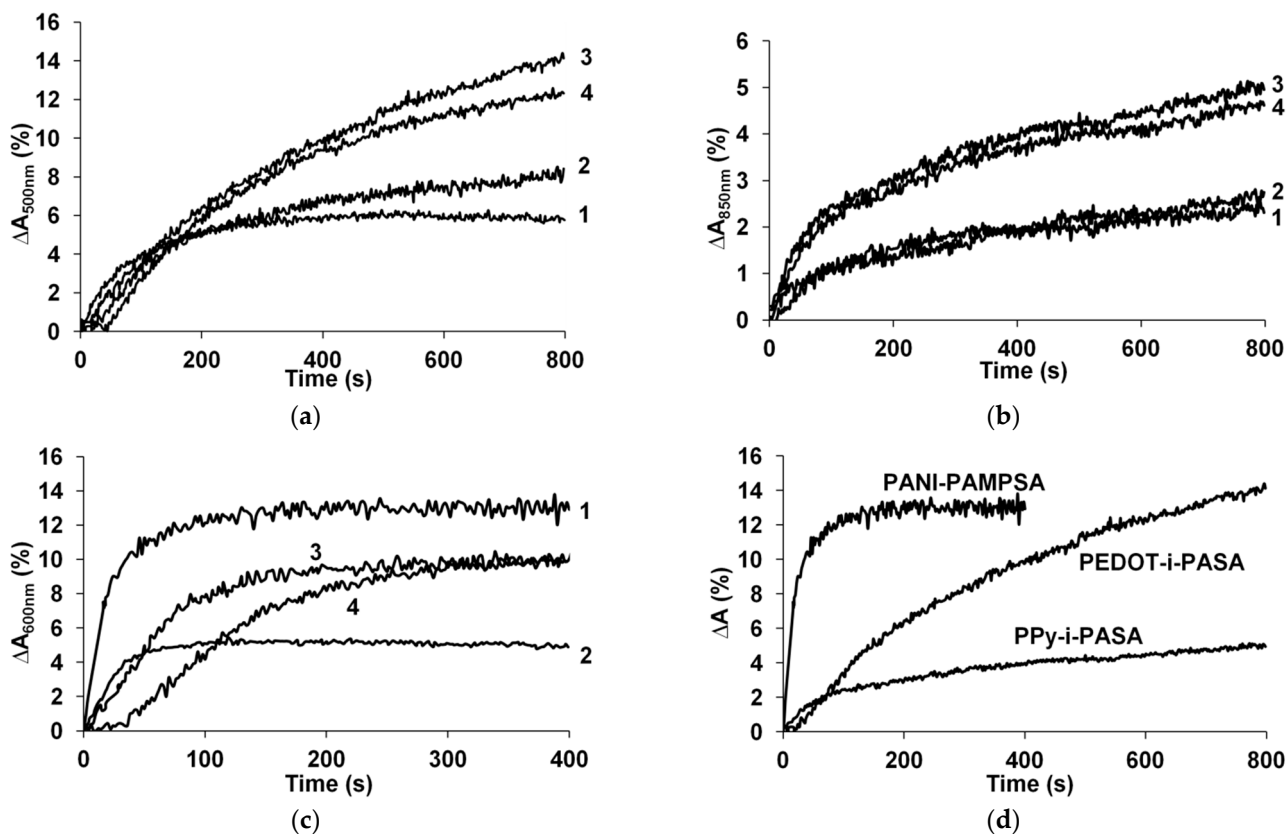


Figure 3. The responses of PEDOT (a), PPy (b) and PANI (c) films prepared in 1-PAMPSA, 2-PSSA, 3-i-PASA and 4-t-PASA exposed to 52 ppm NH_3 . Comparison of the responses of the best CP complexes exposed to 52 ppm NH_3 (d).

For PPy and PEDOT (Figure 4a,b), the saturation of ammonia sorption appeared after 52 ppm. In the case of PANI (Figure 4c, except for PANI-PSSA complex), the growth of ΔA continued up to higher ammonia concentrations (135 ppm), yet with lower slope. This may have been connected with the different mechanisms (reduction or deprotonation) of interaction of different CPs with NH_3 .

To summarize, it can be clearly seen from Figures 3b and 4b that PPy complexes demonstrated poor ΔA and longer response times as compared to PEDOT and PANI films. PEDOT complexes had the highest ΔA in the range of ammonia concentrations less than 52 ppm, while PANI complexes (except for PANI-PSSA) demonstrated reliable NH_3 detection in the widest range of concentrations up to 135 ppm with the shortest response time (Table 1).

The second important parameter was the response time, which depends on the diffusion coefficient of the analyte in the sensor material. Using the time dependences of the change in the optical absorption at the chosen wavelengths, the value of the ammonia diffusion coefficient can be calculated from Equation (3).

Figure 5 shows the dependences of $(A_t - A_0) / (A_k - A_0)$ on $t^{0.5}$. $D^{0.5}$ was found from the slope of these dependences in the linear fragments indicated in the figure. The deviation of the graph from linearity at shorter and longer times indicates the deviation of ammonia diffusion from Fick's second law. As a rule, this is associated with relaxation processes accompanying the diffusion of sorbate in the polymer, which manifest themselves in the

changes in the polymer conformation or structure due to deprotonation and/or reduction of CPs upon interaction with ammonia.

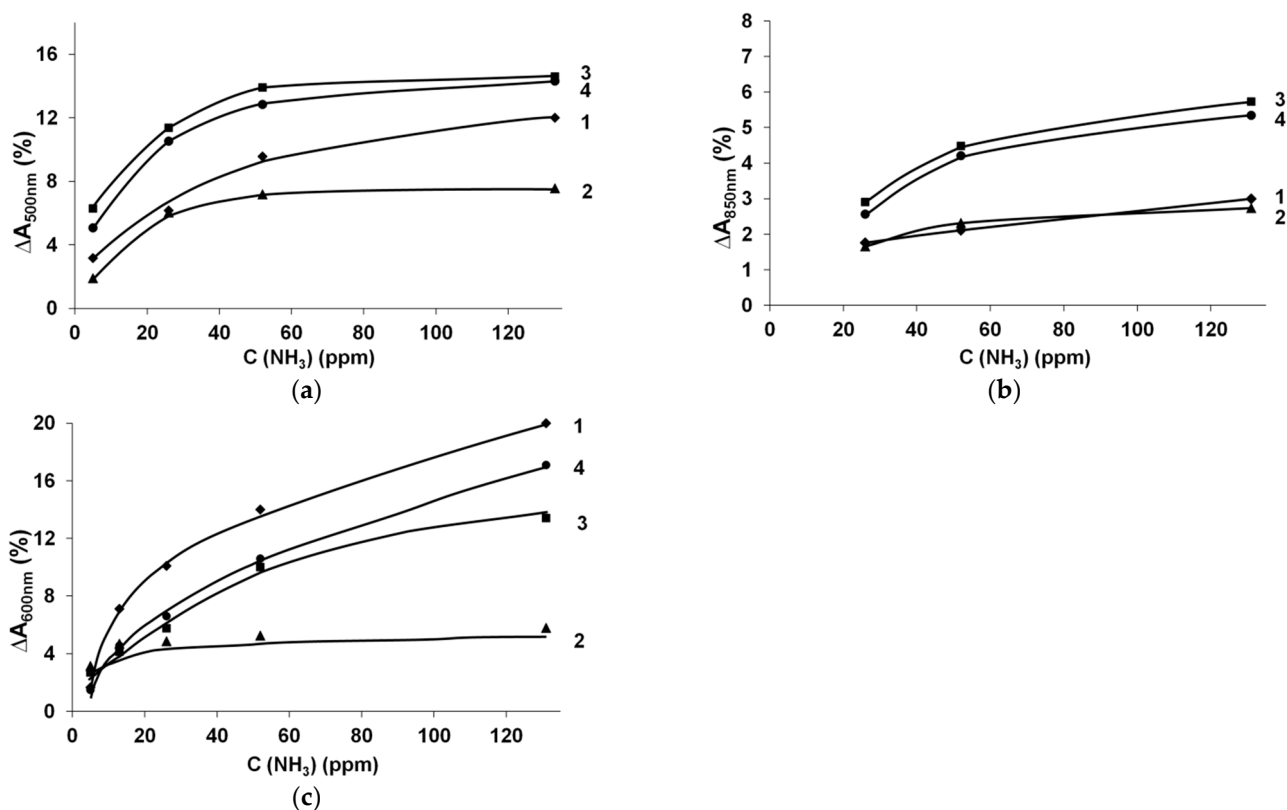


Figure 4. Dependence of response amplitude on the concentration of ammonia for the films of the PEDOT (a), PPy (b) and PANI (c) complexes with 1-PAMPSA, 2-PSSA, 3-i-PASA and 4-t-PASA.

According to the World Health Organization, the workplace exposure limit for ammonia in the air (8 h TWA reference period) is 25 ppm [43]. Therefore, we compared the sensing properties (response amplitude, response time, diffusion coefficient) of the complexes of PEDOT, PPy and PANI at this ammonia concentration threshold (Table 1).

It can be seen that the films of the PANI-PAMPSA and PANI-t-PASA complexes were characterized by the highest diffusion coefficients. As expected, all PPy complexes had the lowest diffusion coefficients and the longest response times. On the other hand, PEDOT complexes had long response times very similar to those of PPy, but with higher ΔA and diffusion coefficients. The latter were closer to the values for PANI complexes but the response of PANI films was significantly faster. Therefore, it can be concluded that not only ammonia diffusion but also the interaction mechanism of CPs with NH₃ affect the sensing properties.

In the majority of studies describing CP-based ammonia sensors [2,3,11,12], the detection range from 20–500 ppm was studied. Sensors operated via a chemiresistive transducing mechanism demonstrated, in general, lower detection limits from 1 ppm [2]. For optical sensors, the detection limits were 12 ppm (PPy dye doped [8]), 2.73 ppm (PEDOT [13]) and 5 ppm (PANI [11]).

The chemiresistive sensors based on CPs have, in general, shorter response times than the optical sensors: PEDOT—10 s at 100 ppm, PPy—15–20 s at 20 ppm, PANI—30 s at 25 ppm [2]. However, an adequate comparison of this parameter with the values obtained in the present study is difficult due to the differences in the thicknesses, detection ranges and response-linearity ranges used in different studies. Also, one should not forget that most of the cited results were obtained for CPs doped with low-molecular acids or salts, which may be evaporated or leached (for example, by dew) from the films, resulting in

unstable sensing characteristics. This is not the case for the polyelectrolyte-doped CPs described in this study.

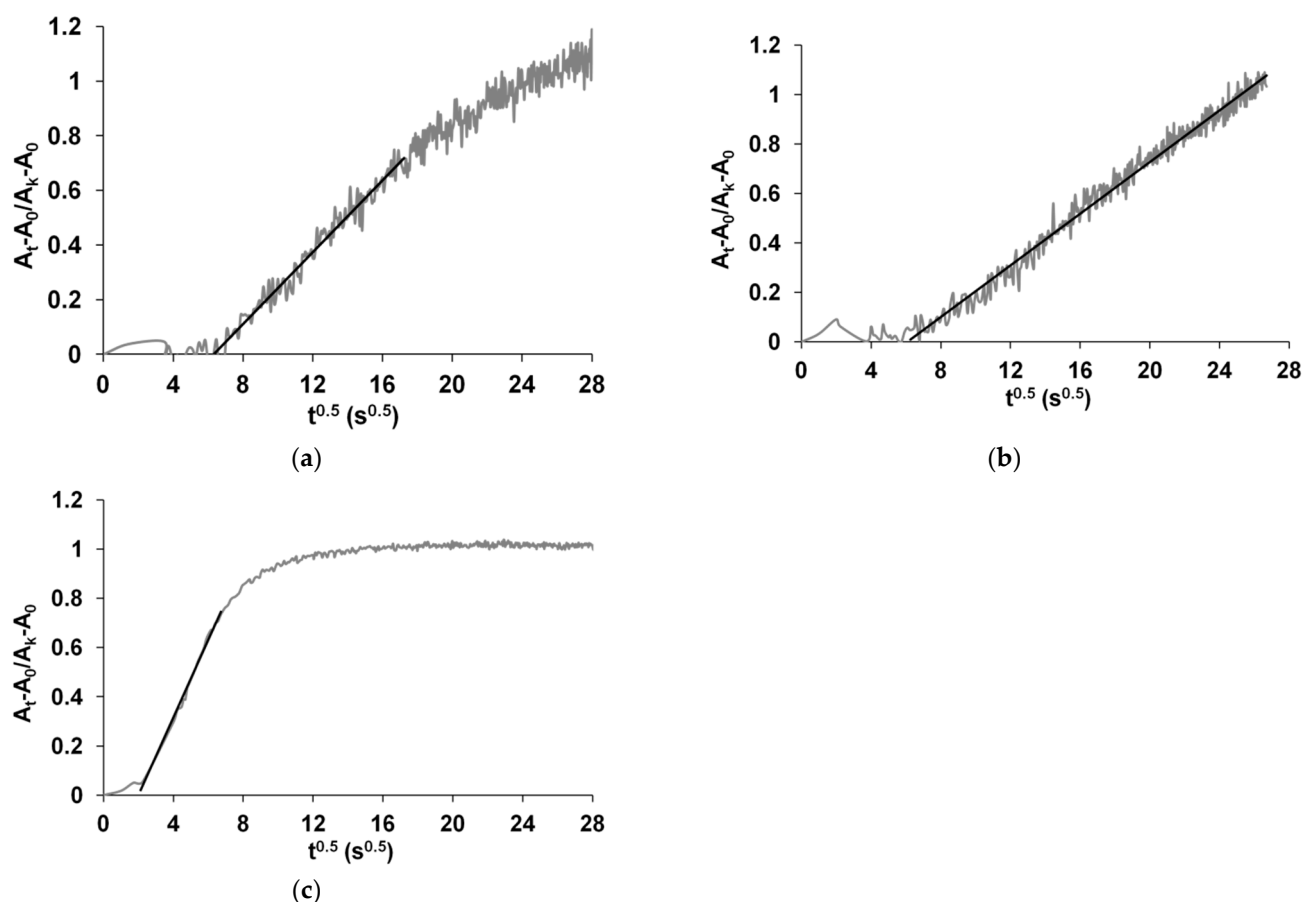


Figure 5. The dependences of $(A_t - A_0) / (A_k - A_0)$ on $t^{0.5}$ for PEDOT-t-PASA (a), PPy-t-PASA (b) and PANI-PAMPSA (c) at 25 ppm of ammonia.

Table 1. Values of the sensor response amplitude (ΔA), response time (t_r) and diffusion coefficient (D) at 25 ppm of ammonia and the roughness (R_q) of films electrodeposited in the different mediums.

	ΔA at 25 ppm, %	t_r , s (25 ppm)	R_q , nm	D , 10^{-13} , cm^2/s
PEDOT-PAMPSA	6.17	637	25.3	6.67
PSSA	6.03	594	17.3	15.4
i-PASA	11.36	636	16.9	16.2
t-PASA	10.53	580	10.9	11.1
PPy-PAMPSA	1.76	488	24.6	5.31
PSSA	1.66	445	21.2	5.65
i-PASA	2.91	574	9.95	2.68
t-PASA	2.56	762	15.5	3.9
PANI-PAMPSA	10.10	81	41.2	66.5
PSSA	4.86	57	9.7	14.7
i-PASA	5.75	170	16.3	22.7
t-PASA	6.60	123	29.1	54.5

3.3. Morphology of CP Films

In a great number of studies, the morphology or surface structure of CPs is denoted as the crucial factor affecting the sensor performance [2,8,10,33,44,45]. High roughness can enhance sensor response by providing high surface-to-volume ratios to enhance the

diffusion of NH_3 molecules and increase the surface contacting the gas molecules [10]. In [10,44,45], it was suggested that the globular nanostructured layers demonstrate larger responses than nanofiber-based ones. The smaller diameters of globules provide higher specific surface areas for gas sorption [8,33].

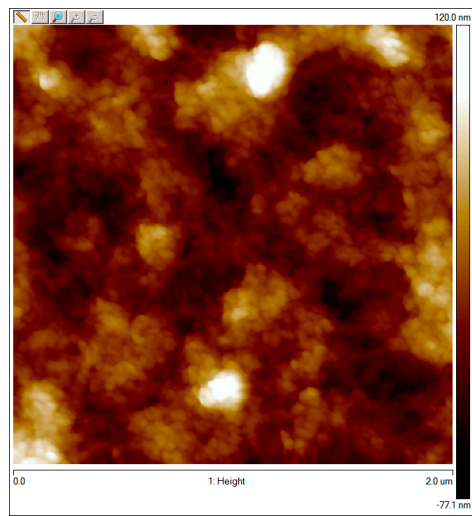
In our work, PEDOT complexes with flexible-chain polyacids had filament-like structures (Figure 6a,b). In contrast, the surfaces of PEDOT with rigid-chain polyacids consisted of isolated globules with small dimensions (especially t-PASA) (Figure 6d). This correlates with their higher response amplitude. All PPy complexes had globular morphologies. The size of the globules was lower in the case of PPy complexes with rigid-chain polyacids (Figure 6g,h) and they had a higher response. So, in the case of CPs preferentially interacting with ammonia through the reduction mechanism, the morphology plays an important role in sensing. In the case of PANI, no such correlation was observed. It can be seen that the PANI complex with PAMPSA had a filament-like structure (Figure 6i) with large dimensions for its elements and high roughness (Table 1). This film demonstrated the best sensing properties. At the same time, the PANI with another flexible-chain polyacid, PSSA (Figure 6j), consisted of small globules, had low roughness and demonstrated the worst response. PANI complexes with rigid-chain polyacids demonstrated good responses comparable with PANI-PAMPSA, but they had a different morphology. The surface of PANI-i-PASA (Figure 6k) consisted of isolated globules that were larger than those for PANI-PSSA, whereas PANI-t-PASA had a filament-like structure (Figure 6l). Therefore, for CPs interacting with ammonia through a combined reduction and deprotonation mechanism, the morphology was not very significant for the ammonia-sensing performance. Proton transport by hopping via sulfonic sites inside the film, which is discussed below, seemed to be more important.

3.4. Specific Features of Sensing Properties of CP Polyacid Films

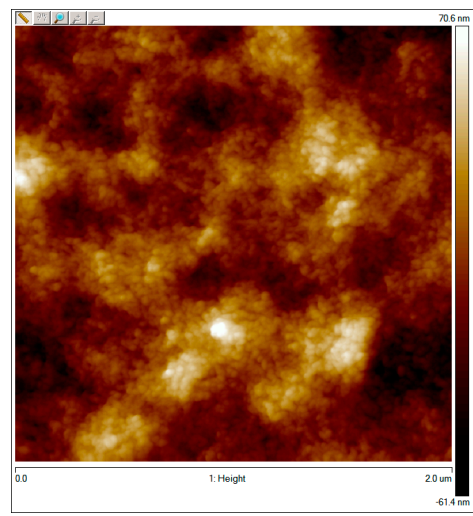
Some interesting features of the sensing properties of PPy complexes with polyelectrolytes in the acid or salt forms were found in [16]. The first feature is that the protons in the films of PPy polyacid complexes can easily migrate via the sulfonic acid sites to the film surface, where they can react with ammonia molecules, resulting in a more rapid sensing response of PPy polyacid films as compared to PPy polysalt ones. In these conditions, the film is deprotonated more deeply and the spectral changes occur both in the surface areas and in the bulk of the film. A similar mechanism was found to be responsible for the more intensive and rapid sensing response of PANI polyacid complexes in this work.

Since the conductivity of CP depends on the degree of oxidation, the reducing effect of ammonia vapors can cause the propagation of the reduction front from the film surface to its bulk. Similar phenomena may have affected the ammonia-sensing properties of PEDOT polyacid complexes in this work.

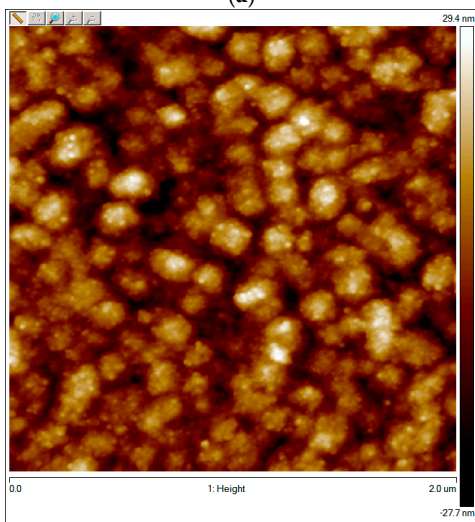
Another important feature is the possible neutralization of a part of the ammonia molecules by excessive protons of polyacids. The acceleration of the sensing response of PPy polyacid films after their treatment in CaCl_2 was shown in [16]. This treatment leads to cross-linking of the polyacid matrix [46] by strong ionic bonds of Ca^{2+} ions, with two sulfogroups belonging to adjacent polyacid chains. This results in effective replacement of excessive protons. In this study, this experiment was also repeated for PEDOT and PANI films. As expected, in the case of PEDOT complexes no changes in ΔA and response time were observed due to the purely reductive mechanism of their interaction with ammonia, and some reduction of ΔA was even observed (Figure 7a).



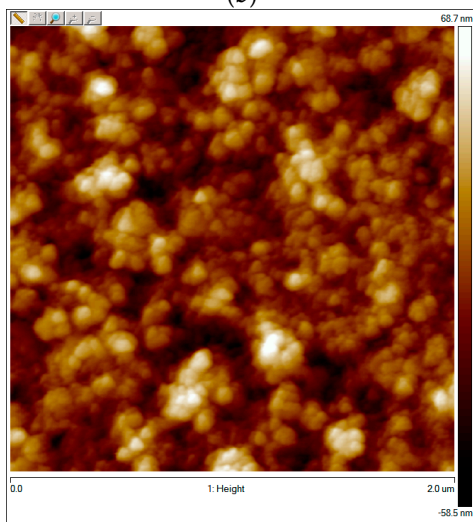
(a)



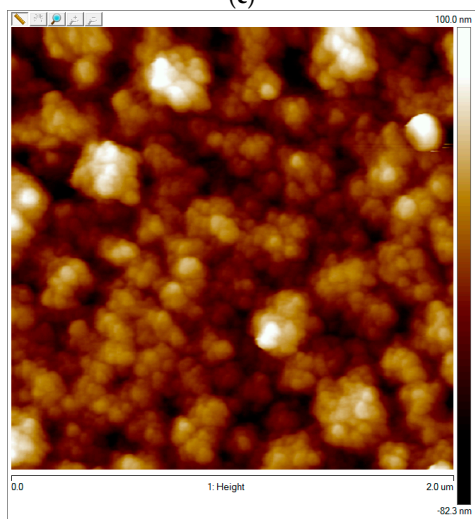
(b)



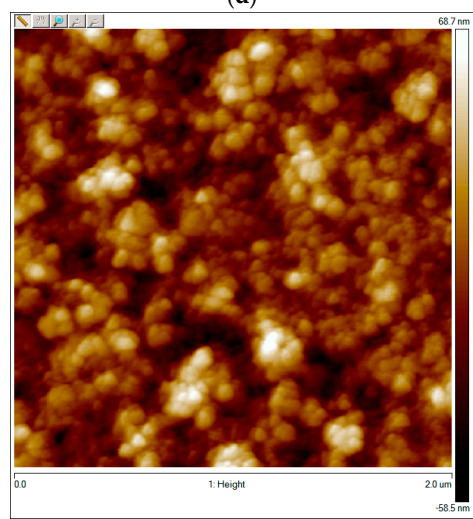
(c)



(d)



(e)



(f)

Figure 6. Cont.

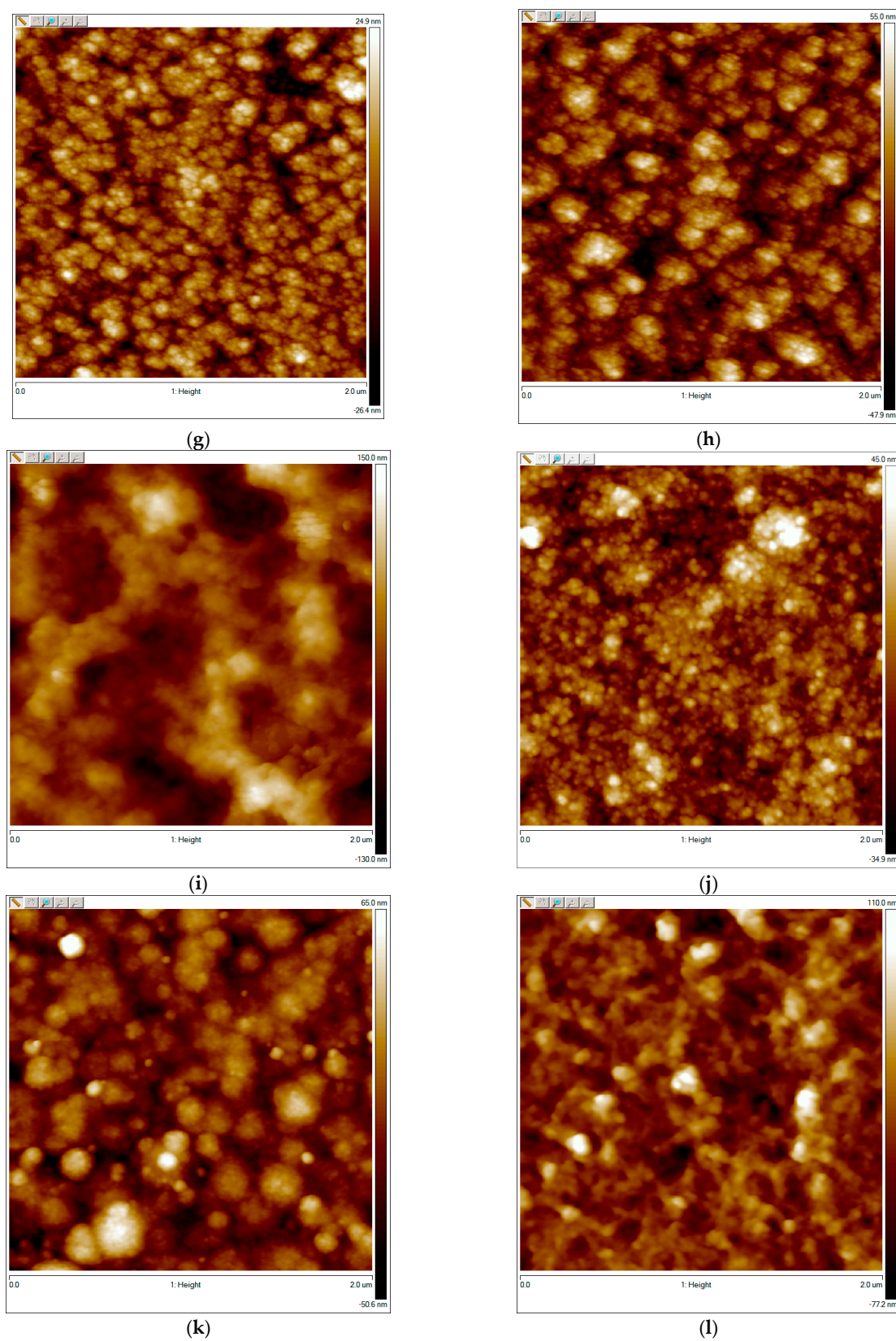


Figure 6. AFM images of PEDOT films obtained in PAMPSA (a), PSSA (b), i-PASA (c) and t-PASA (d); PPy films obtained in PAMPSA (e), PSSA (f), i-PASA (g) and t-PASA (h); and PANI films obtained in PAMPSA (i), PSSA (j), i-PASA (k) and t-PASA (l).

The sensing responses of CaCl_2 -treated PANI films to NH_3 are presented in Figure 7b,c. A higher response amplitude (about 1.5–2 times) in the case of CaCl_2 -treated PANI-PAMPSA and PANI-t-PASA films can be seen. The relative decrease in the response time was more obvious for the PANI-t-PASA complex (1.3 times). Thus, in the absence of an excess of protons, especially on the film surface, most of the ammonia molecules react with protonated PANI (similarly to PPy). In the case of PPy, the neutralization of excessive protons only influenced the response time [16]. So, the deprotonation of the PPy surface occurs at an early stage and then the amplitude of PPy response is largely determined by its reduction. In the case of PANI, the growth of the response amplitude of the complexes, both with the rigid- and flexible-chain polyacids, and the decrease of the response time of the PANI-t-PASA film can be seen. Short and straight molecules of t-PASA are probably not excessively trapped in the film during the synthesis and have more accessible protonated sulfoacid groups on the film surface, which may neutralize ammonia at the initial stage. Accordingly, the sulfoacid groups of rigid-chain t-PASA are more accessible for treatment with CaCl_2 , which results in a more significant increase in the response amplitude and decrease in the response time for PANI-t-PASA films.

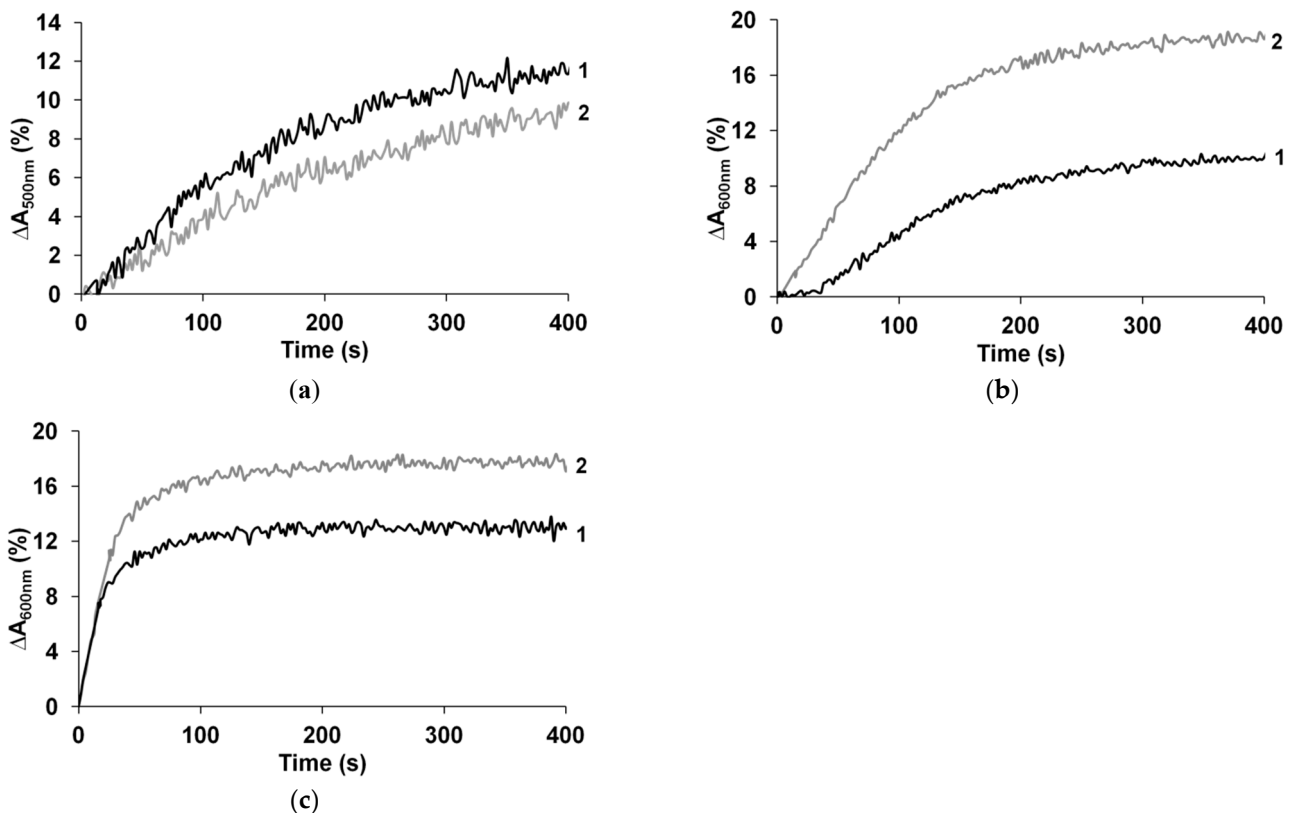


Figure 7. Influence of excessive proton replacement on the sensing properties of PEDOT-t-PASA (a), PANI-t-PASA (b) and PANI-PAMPSA (c) 1—as prepared, 2—treated in 10% CaCl_2 , exposed to 52 ppm NH_3 .

In [2], it was noted that PANI seems to be a more suitable material for the detection of NH_3 and it frequently possessed higher responses than other conducting polymers [3]. The fast process of PANI deprotonation [41] and the developed surface structure with high porosity lead to its good sensing properties. We assumed that the structural changes during reduction of CP comprise a slower process than deprotonation, particularly if there is a possibility of proton transport from the bulk of the film. As a result, PEDOT has a longer response time. Due to the fact that PPy has a lower range of optical changes during reduction/oxidation [22] than PEDOT [23] and, during protonation/deprotonation [39], than PANI [41], it demonstrates lower ΔA . However, it is not only the nature of CPs that influences sensor performance.

The flexibility and structure of polyacid chains play important roles in the formation of the bulk structure of CPs. The PANI complex with PSSA had possibly the worst sensing properties among the PANI complexes due to its having the lowest roughness (Table 1). Moreover, it has been shown by XPS analysis that the PANI-PSSA complex has a lower doping level (the ratio between changed nitrogen atoms and the total amount of nitrogen) [26]. Therefore, it has a lower amount of changed nitrogen atoms capable of donating protons to ammonia.

It has been shown that PEDOT [23] and PPy [22] films obtained in the presence of more rigid-chain amide-containing polyacids are characterized by low doping levels and retarded formation of bipolaronic fragments. Therefore, the reduction of PEDOT and PPy under the influence of ammonia proceeds preferentially through a single transition from the first oxidized state (polaronic) to the reduced state. For this reason, PEDOT and PPy complexes with rigid-chain polyacids have a higher ΔA than the complexes with flexible chain polyacids, in which formation of the second oxidized state (bipolaronic) is more probable.

3.5. Regeneration

CP gas sensors based on conductivity measurement can only be partly regenerated by passing air or nitrogen gas through the sensor to remove the ammonia adsorbed on the surface [10]. However, there is no information about complete regeneration of PEDOT films. It was shown in [38] that PPy cannot be completely regenerated after exposure to NH_3 . The authors of [10] reported the presence of trapped NH_3 molecules in the layers of PANI that were not completely desorbed during the regeneration process.

An effective method for regenerating a sensor, in which the sensor is heated up to 120°C , was proposed in [42]. Regeneration via treatment with a dilute hydrochloric acid solution at room temperature has been used for an optical ammonia sensor based on PANI [9,10] but it is not convenient from a practical point of view.

In our opinion, thermal treatment via resistive heating of the conducting layer (FTO or ITO) on which the CP films are deposited is the most suitable method for regeneration of optical ammonia sensors. The process of regeneration of the PANI-PAMPSA film is presented in Figure 8. PANI film regeneration in air (a) for 25 min led to a 50% restoration of its spectrum. It was restored almost completely after a day in air. Resistive heating of the conductive, optically transparent, FTO layer (b) up to $\sim 75^\circ\text{C}$ removed ammonia from the film at a higher rate. It can be clearly seen that $\sim 70\%$ of the response amplitude of the PANI film was regenerated in 15 min.

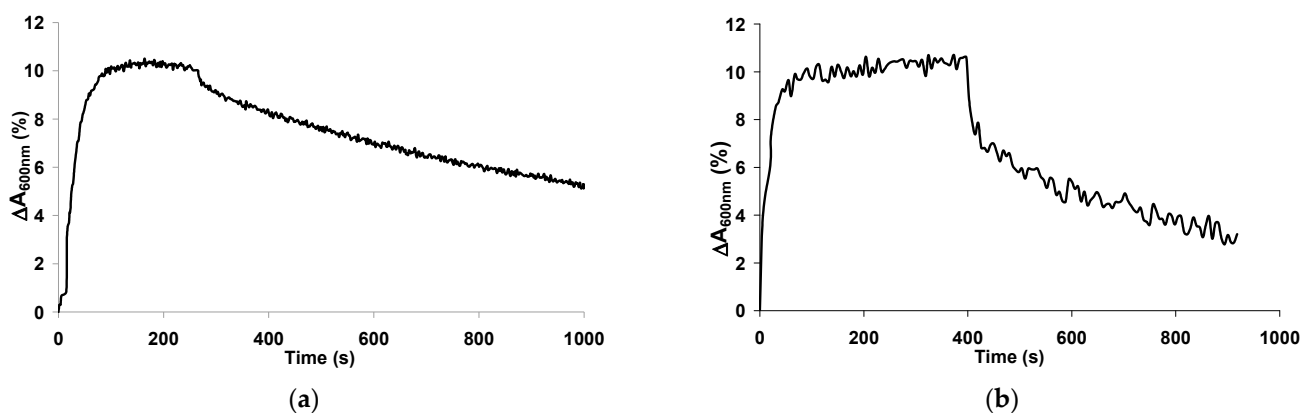


Figure 8. The response of PANI-PAMPSA film exposed to 52 ppm of ammonia and its regeneration in air (a) and via resistive heating of the FTO layer (b).

4. Conclusions

In this article, we first presented a comparative study of the optical sensing properties of conducting polymer (PEDOT, polypyrrole, polyaniline) complexes with polysulfonic acids of different structures and chain flexibilities. A range of ammonia vapor concentrations from 5 to 135 ppm was studied.

It was shown that the response amplitude, response time and ammonia diffusion coefficient were dependent on the dominant mechanism of interaction (reduction and/or deprotonation) of the conducting polymers with the ammonia, flexibility and structure of polyacid chains used during their electrosynthesis.

The following specific features were discovered:

1. CP-polyacid films with a deprotonation mechanism could more rapidly respond to ammonia because the hydrogen ions could easily migrate via sulfoacid sites from the bulk to the surface of the film, causing deprotonation in the deeper areas of the film. This resulted in deeper spectral changes;
2. The presence of excessive protons of polyacid in the films decreased their optical response amplitude and increased the response time due to partial neutralization of ammonia by these excessive protons. This phenomenon could be eliminated by treatment of the films in CaCl_2 , resulting in cross-linking of sulfogroups from adjacent polyacid chains by Ca^{2+} ions;
3. In the case of CPs with a preference for a reduction mechanism of sensing (PEDOT, PPy), the complexes with rigid-chain polyacids exhibited higher amplitudes of optical response than the complexes with flexible-chain polyacids. This was due to the fact that their reduction proceeded mainly via a single transition from the first oxidized state (polaronic) to the reduced state;
4. In the case of CPs with a preference for a deprotonation mechanism of sensing (PANI), a high—and the most rapid—optical response was observed independently of the structure of the polyacid dopant and the morphology of the PANI polyacid films. Surprisingly, the PANI complex with the popular PSSA demonstrated the worst sensing properties.

Thermal treatment by resistive heating of the conducting layer (FTO) on which the PANI films were electrodeposited was successfully tested for regeneration of the optical sensors for ammonia vapors.

Author Contributions: Conceptualization: O.G. and A.N.; experimental investigation: V.K. and O.G.; data analysis and interpretation: O.G. and V.T.; writing—original draft preparation: O.G.; writing—review and editing: A.N.; supervision: A.N.; project administration: A.N.; funding acquisition: IPCE RAS. All authors have read and agreed to the published version of the manuscript.

Funding: This study was financially supported by the Ministry of Science and Higher Education of the Russian Federation (federal contract of IPCE RAS).

Institutional Review Board Statement: Not applicable.

Informed Consent Statement: Not applicable.

Data Availability Statement: Not applicable.

Acknowledgments: The AFM measurements were performed using equipment from CKP FMI IPCE RAS.

Conflicts of Interest: The authors declare no conflict of interest. The funders had no role in the design of the study; in the collection, analyses, or interpretation of data; in the writing of the manuscript; or in the decision to publish the results.

References

1. Bai, H.; Shi, G. Gas sensors based on conducting polymers. *Sensors* **2007**, *7*, 267–307. [[CrossRef](#)]
2. Wong, Y.C.; Ang, B.C.; Haseeb, A.S.M.A.; Baharuddin, A.A.; Wong, Y.H. Review—Conducting Polymers as Chemiresistive Gas Sensing Materials: A Review. *J. Electrochem. Soc.* **2020**, *167*, 037503. [[CrossRef](#)]

3. Lakard, B.; Carquigny, S.; Segut, O.; Patois, T.; Lakard, S. Gas Sensors Based on Electrodeposited Polymers. *Metals* **2015**, *5*, 1371–1386. [[CrossRef](#)]
4. Lange, U.; Roznyatovskaya, N.V.; Mirsky, V.M. Conducting polymers in chemical sensors and arrays. *Anal. Chim. Acta* **2008**, *614*, 1–26. [[CrossRef](#)]
5. Su, P.-G.; Lee, C.-T.; Chou, C.-Y. Flexible NH₃ sensors fabricated by in situ self-assembly of polypyrrole. *Talanta* **2009**, *80*, 763–769. [[CrossRef](#)]
6. Wang, S.; Liu, B.; Duan, Z.; Zhao, Q.; Zhang, Y.; Xie, G.; Jiang, Y.; Li, S.; Tai, H. PANI nanofibers-supported Nb₂CT_x nanosheets-enabled selective NH₃ detection driven by TENG at room temperature. *Sens. Actuators B Chem.* **2021**, *327*, 128923. [[CrossRef](#)]
7. Zhang, Y.; Zhang, J.; Jiang, Y.; Duan, Z.; Liu, B.; Zhao, Q.; Wang, S.; Yuan, Z.; Tai, H. Ultrasensitive flexible NH₃ gas sensor based on polyaniline/SrGe₄O₉ nanocomposite with ppt-level detection ability at room temperature. *Sens. Actuators B Chem.* **2020**, *319*, 128293. [[CrossRef](#)]
8. Tavoli, F.; Alizadeh, N. Optical ammonia gas sensor based on nanostructure dye-doped polypyrrole. *Sens. Actuators B Chem.* **2013**, *176*, 761–767. [[CrossRef](#)]
9. Jin, Z.; Su, Y.; Duan, Y. Development of a polyaniline-based optical ammonia sensor. *Sens. Actuators B Chem.* **2001**, *72*, 75–79. [[CrossRef](#)]
10. Kebiche, H.; Debarnot, D.; Merzouki, A.; Poncin-Epaillard, F.; Haddaoui, N. Relationship between ammonia sensing properties of polyaniline nanostructures and their deposition and synthesis methods. *Anal. Chim. Acta* **2012**, *737*, 64–71. [[CrossRef](#)] [[PubMed](#)]
11. Duboriz, I.; Pud, A. Polyaniline/poly(ethylene terephthalate) film as a new optical sensing material. *Sens. Actuators B Chem.* **2014**, *190*, 398–407. [[CrossRef](#)]
12. Christie, S.; Scorsone, E.; Persaud, K.; Kvasnik, F. Remote detection of gaseous ammonia using the near infrared transmission properties of polyaniline. *Sens. Actuators B Chem.* **2003**, *90*, 163–169. [[CrossRef](#)]
13. Ismail, A.H.; Mohd Yahya, N.A.; Yaacob, M.H.; Mahdi, M.A.; Sulaiman, Y. Optical ammonia gas sensor of poly(3,4-polyethylenedioxythiophene), polyaniline and polypyrrole: A comparative study. *Synth. Met.* **2020**, *260*, 116294. [[CrossRef](#)]
14. Ismail, A.H.; Mohd Yahya, N.A.; Mahdi, M.A.; Yaacob, M.H.; Sulaiman, Y. Gasochromic response of optical sensing platform integrated with polyaniline and poly(3,4-ethylenedioxythiophene) exposed to NH₃ gas. *Polymer* **2020**, *192*, 122313. [[CrossRef](#)]
15. Carquigny, S.; Sanchez, J.B.; Berger, F.; Lakard, B.; Lallemand, F. Ammonia gas sensor based on electrosynthesized polypyrrole films. *Talanta* **2009**, *78*, 199–206. [[CrossRef](#)]
16. Gribkova, O.L.; Kabanova, V.A.; Nekrasov, A.A. Electrodeposition of thin films of polypyrrole-polyelectrolyte complexes and their ammonia-sensing properties. *J. Solid State Electrochem.* **2020**, *24*, 3091–3103. [[CrossRef](#)]
17. Łapkowski, M. Electrochemical synthesis of polyaniline/poly(2-acryl-amido-2-methyl-1-propane-sulfonic acid) composite. *Synth. Met.* **1993**, *55*, 1558–1563. [[CrossRef](#)]
18. Hyodo, K.; Nozaki, M. High ion selective electrochemical synthesis of polyaniline. *Electrochim. Acta* **1988**, *33*, 165–166. [[CrossRef](#)]
19. Gustafsson, J.; Liedberg, B.; Inganas, O. In situ spectroscopic investigations of electrochromism and ion transport in a poly(3,4-ethylenedioxythiophene) electrode in a solid state electrochemical cell. *Solid State Ion.* **1994**, *69*, 145–152. [[CrossRef](#)]
20. Bobacka, J.; Lewenstam, A.; Ivaska, A. Electrochemical impedance spectroscopy of oxidized poly(3,4-ethylenedioxythiophene) film electrodes in aqueous solutions. *J. Electroanal. Chem.* **2000**, *489*, 17–27. [[CrossRef](#)]
21. Shimidzu, T.; Ohtani, A.; Iyoda, T.; Honda, K. Charge-controllable polypyrrole/polyelectrolyte composite membranes. Part II. Effect of incorporated anion size on the electrochemical oxidation-reduction process. *J. Electroanal. Chem.* **1987**, *224*, 123–135. [[CrossRef](#)]
22. Gribkova, O.L.; Kabanova, V.A.; Iakobson, O.D.; Nekrasov, A.A. Spectroelectrochemical investigation of electrodeposited polypyrrole complexes with sulfonated polyelectrolytes. *Electrochim. Acta* **2021**, *382*, 138307. [[CrossRef](#)]
23. Gribkova, O.L.; Iakobson, O.D.; Nekrasov, A.A.; Cabanova, V.A.; Tverskoy, V.A.; Tameev, A.R.; Vannikov, A.V. Ultraviolet-Visible-Near Infrared and Raman spectroelectrochemistry of poly(3,4-ethylenedioxythiophene) complexes with sulfonated polyelectrolytes. The role of inter- and intra-molecular interactions in polyelectrolyte. *Electrochim. Acta* **2016**, *222*, 409–420. [[CrossRef](#)]
24. Nekrasov, A.A.; Gribkova, O.L.; Eremina, T.V.; Isakova, A.A.; Ivanov, V.F.; Tverskoj, V.A.; Vannikov, A.V. Electrochemical synthesis of polyaniline in the presence of poly(amidosulfonic acid)s with different rigidity of polymer backbone and characterization of the films obtained. *Electrochim. Acta* **2008**, *53*, 3789–3797. [[CrossRef](#)]
25. Gribkova, O.L.; Nekrasov, A.A.; Ivanov, V.F.; Zolotarevsky, V.I.; Vannikov, A.V. Templating effect of polymeric sulfonic acids on electropolymerization of aniline. *Electrochim. Acta* **2014**, *122*, 150–158. [[CrossRef](#)]
26. Lyutov, V.; Kabanova, V.; Gribkova, O.; Nekrasov, A.; Tsakova, V. Electrochemically-Obtained Polysulfonic-Acids Doped Polyaniline Films—A Comparative Study by Electrochemical, Microgravimetric and XPS Methods. *Polymers* **2020**, *12*, 1050. [[CrossRef](#)]
27. Lyutov, V.; Ivanov, S.; Mirsky, V.; Tsakova, V. Polyaniline doped with poly(acrylamidomethylpropanesulphonic acid): Electrochemical behaviour and conductive properties in neutral solutions. *Chem. Pap.* **2013**, *67*, 1002–1011. [[CrossRef](#)]
28. Lyutov, V.; Efimov, I.; Bund, A.; Tsakova, V. Electrochemical polymerization of 3,4-ethylenedioxythiophene in the presence of dodecylsulfate and polysulfonic anions—An acoustic impedance study. *Electrochim. Acta* **2014**, *122*, 21–27. [[CrossRef](#)]
29. Kirsh, Y.E.; Fedotov, Y.A.; Iudina, N.A.; Artemov, D.Y.; Nekrasova, T.N. Polyelectrolyte properties of sulphur-containing polyamides based on isophthalic and terephthalic acids in aqueous solutions. *Polym. Sci. USSR* **1991**, *33*, 1040–1047. [[CrossRef](#)]

30. Rabinovich, V.A.; Yakovlevich, K.Z. *Kratkii Khimicheskii Spravochnik (Short Chemical Handbook)*; Khimiya: Moscow, Russia, 1977.
31. Chen, J.; Lotfi, A.; Hesketh, P.J.; Kumar, S. Carbon nanotube thin-film-transistors for gas identification. *Sens. Actuators B Chem.* **2019**, *281*, 1080–1087. [[CrossRef](#)]
32. Anwane, R.S.; Kondawar, S.B.; Late, D.J. Bessel's polynomial fitting for electrospun polyacrylonitrile/polyaniline blend nanofibers based ammonia sensor. *Mater. Lett.* **2018**, *221*, 70–73. [[CrossRef](#)]
33. Zhang, Y.; Kim, J.J.; Chen, D.; Tuller, H.L.; Rutledge, G.C. Electrospun Polyaniline Fibers as Highly Sensitive Room Temperature Chemiresistive Sensors for Ammonia and Nitrogen Dioxide Gases. *Adv. Funct. Mater.* **2014**, *24*, 4005–4014. [[CrossRef](#)]
34. Tager, A.A. *Physicochemistry of Polymers (4th Edition, Revised and Supplemented)*; Scientific World: Moscow, Russia, 2007; ISBN 978-589-176-437-8.
35. Łapkowski, M.; Proń, A. Electrochemical oxidation of poly(3,4-ethylenedioxythiophene)—“in situ” conductivity and spectroscopic investigations. *Synth. Met.* **2000**, *110*, 79–83. [[CrossRef](#)]
36. Kwon, O.S.; Park, E.; Kweon, O.Y.; Park, S.J.; Jang, J. Novel flexible chemical gas sensor based on poly(3,4-ethylenedioxythiophene) nanotube membrane. *Talanta* **2010**, *82*, 1338–1343. [[CrossRef](#)]
37. Jang, J.; Chang, M.; Yoon, H. Chemical Sensors Based on Highly Conductive Poly(3,4-ethylenedioxythiophene) Nanorods. *Adv. Mater.* **2005**, *17*, 1616–1620. [[CrossRef](#)]
38. Gustafsson, G.; Lundström, I.; Liedberg, B.; Wu, C.R.; Inganäs, O.; Wennerström, O. The interaction between ammonia and poly(pyrrole). *Synth. Met.* **1989**, *31*, 163–179. [[CrossRef](#)]
39. Qian, R.; Pei, Q.; Huang, Z. The role of H⁺ ions in the electrochemical polymerization of pyrrole. *Die Makromol. Chem.* **1991**, *192*, 1263–1273. [[CrossRef](#)]
40. Nekrasov, A.A.; Ivanov, V.F.; Vannikov, A.V. Analysis of the structure of polyaniline absorption spectra based on spectroelectrochemical data. *J. Electroanal. Chem.* **2000**, *482*, 11–17. [[CrossRef](#)]
41. Stejskal, J.; Kratochvíl, P.; Radhakrishnan, N. Polyaniline dispersions 2. UV—Vis absorption spectra. *Synth. Met.* **1993**, *61*, 225–231. [[CrossRef](#)]
42. Kukla, A.L.; Shirshov, Y.M.; Piletsky, S.A. Ammonia sensors based on sensitive polyaniline films. *Sens. Actuators B Chem.* **1996**, *37*, 135–140. [[CrossRef](#)]
43. Health and Safety Executive EH40/2005. Workplace exposure limits limits for use with the Control of Substances (Fourth Edition 2020). *Tso* **2020**, *2002*, 61.
44. Wojkiewicz, J.L.; Bliznyuk, V.N.; Carquigny, S.; Elkamchi, N.; Redon, N.; Lasri, T.; Pud, A.A.; Reynaud, S. Nanostructured polyaniline-based composites for ppb range ammonia sensing. *Sens. Actuators B Chem.* **2011**, *160*, 1394–1403. [[CrossRef](#)]
45. Kumar, L.; Rawal, I.; Kaur, A.; Annapoorni, S. Flexible room temperature ammonia sensor based on polyaniline. *Sens. Actuators B Chem.* **2017**, *240*, 408–416. [[CrossRef](#)]
46. Gribkova, O.L.; Nekrasov, A.A.; Trchova, M.; Ivanov, V.F.; Sazikov, V.I.; Razova, A.B.; Tverskoy, V.A.; Vannikov, A.V. Chemical synthesis of polyaniline in the presence of poly(amidosulfonic acids) with different rigidity of the polymer chain. *Polymer* **2011**, *52*, 2474–2484. [[CrossRef](#)]